Empirical Wind Turbine Load Distributions Using Field Data

Puneet Agarwal
Graduate Research Assistant
e-mail: pagarwal@mail.utexas.edu

Lance Manuel[1]
Associate Professor
e-mail: lmanuel@mail.utexas.edu

Department of Civil, Architectural, and Environmental Engineering, University of Texas, Austin, TX 78712

*In the design of land-based or offshore wind turbines for ultimate limit states, long-term loads associated with return periods on the order of the service life (*20 years*, usually) must be estimated. This requires statistical extrapolation from turbine load data that may be obtained by simulation or by field tests. The present study illustrates such extrapolation that uses field data from the Blyth offshore wind farm in the United Kingdom, where a* 2 MW *wind turbine was instrumented, and environment and load data were recorded. From this measurement campaign, the load data available are in two different formats: as* 10 min *statistics (referred to as "summary" data) or as full time series (referred to as "campaign" data). The characteristics of the site and environment and, hence, that of the turbine response are strikingly different for winds from the sea and winds from the shore. The load data (here, only the mudline bending moment is studied) at the Blyth site are hence separated depending on wind regime. By integrating load distributions conditional on the environment with the relative likelihood of the different environmental conditions, long-term loads associated with specified return periods can be derived. This is achieved here using the peak-over-threshold method based on campaign data but long-term loads are compared with similar estimates based on the summary data. Winds from the shore are seen to govern the long-term loads at the site. Though the influence of wave heights on turbine long-term loads is smaller than that of wind speed, there is possible resonance of tower dynamics induced by the waves; still, to first order, it is largely the wind speed and turbulence intensity that control design loads. Predicted design loads based on the campaign data are close to those based on the summary data discussed in a separate study.* [DOI: 10.1115/1.2827937]

Introduction

Our objective is to estimate design loads for an offshore wind turbine for which the environmental and load data are available from field measurements. Using a probabilistic approach, we intend to estimate design loads associated with a target probability of exceedance or, equivalently, a prescribed service life for the turbine. Variables describing the wind and wave environment as well as the turbine response are modeled as random; their probabilistic distributions need to be established. Available data obtained from full-scale field measurements can provide a more realistic representation of the turbine response subjected to various environmental conditions than is possible with simulation data. Field data, however, can be "limited" in the sense that they are often recorded only for a finite duration of time, and may not systematically cover all possible environmental conditions expected to occur over the life of the turbine. Hence, with such limited data, statistical techniques are often used to extrapolate the loads from observed events to rarer loads associated with prescribed safety levels. Statistical extrapolation has been used to predict both extreme and fatigue design loads for wind turbines. A recent draft from the International Electrotechnical Commission (IEC) [1] of offshore wind turbine design guidelines also recommends its use. Examples of its use in other studies include those by Moriarty et al. [2], Fitzwater and Winterstein [3], and Agarwal and Manuel [4].

Our focus here is on the bending moment at the base of the turbine tower (the mudline bending moment) as the load variable of interest. The turbine under consideration is an instrumented 2 MW wind turbine at the Blyth wind farm, located about 1 km off the northeast coast of England, and for which data were recorded for about 16 months. Key features of the site pertinent to the present study include contrasting characteristics of the environment and response associated with winds blowing from the shore to the sea (winds from the shore) versus those associated with winds blowing from the sea to the shore (winds from the sea). We use the campaign data (available as 10 min time series) to predict long-term design loads. To gain a better understanding, we separate the data into wind regimes associated with winds from the shore and those from the sea as well as divide the data in each regime according to 10 min average wind speed V and significant wave height H_s. Then, for each bin or interval representing different V-H_s combinations, "short-term" load extreme probability distributions are derived using the peak-over-threshold (POT) method. Integration of these short-term load distributions with the likelihood of different V-H_s combinations can help to derive the desired design load. Due to statistical uncertainty associated with the use of limited data, we discuss how nonparametric bootstrap methods can be used to establish confidence intervals on design load predictions. The results from this study based on POT data are compared with those from a separate study that employed global (or epochal) load maxima available from summary data.

Load Extrapolation

Design Load Case 1.1b of the IEC 61400-3 draft design guidelines recommends the use of statistical extrapolation methods to predict extreme turbine loads [1]. With statistical extrapolation for wind turbine extreme loads, one seeks to estimate the turbine design load l_T associated with a target probability of exceedance P_T or equivalently with a target service life of T years, using the following equation:

[1]Corresponding author.

Contributed by the Ocean Offshore and Arctic Engineering Division of ASME for publication in the JOURNAL OF OFFSHORE MECHANICS AND ARCTIC ENGINEERING. Manuscript received July 8, 2007; final manuscript received October 21, 2007. Published online January 29, 2008. Review conducted by: Takeshi Kinoshita. Paper presented at the The 26th International Conference on Offshore Mechanics and Arctic Engineering (OMm,AE2007), San Diego, CA, June 10–15, 2007.

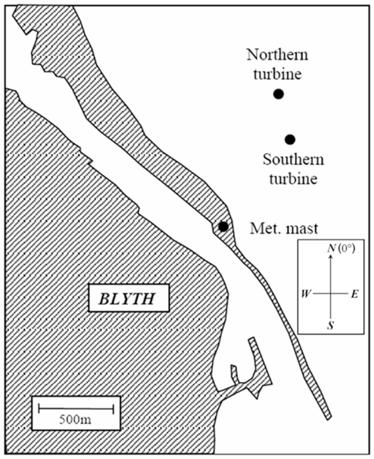

Fig. 1 Location of the turbines and an onshore meteorological mast at the Blyth site (from Camp et al. [5])

$$P_T = P[L > l_T] = \int_{\mathbf{X}} P[L > l_T | \mathbf{X} = \mathbf{x}] f_{\mathbf{X}}(\mathbf{x}) d\mathbf{x} \tag{1}$$

where $f_{\mathbf{X}}(\mathbf{x})$ is the joint probability density function (PDF) of the environmental random variables, $\mathbf{X}$. For different trial values of load l_T, Eq. (1) enables one to compute the long-term probability of exceeding that load by integrating the short-term load exceedance probability conditional on $\mathbf{X}$, namely, $P[L > l_T | \mathbf{X} = \mathbf{x}]$, with the relative likelihood of different environmental conditions, $\mathbf{X}$. One is required to integrate over the entire domain of all random variables—the load level l_T is adjusted until the target probability P_T results from the integration. In this study, the environmental random variables taken to comprise $\mathbf{X}$ are the 10 min mean wind speed V at hub height in the along wind direction and the significant wave height H_s. The short-term load distribution, $P[L > l_T | \mathbf{X} = \mathbf{x}]$, is established for different values of $\mathbf{X}$ by applying the POT method to the campaign data time series.

Blyth Site and Field Data

The Blyth project is an experimental wind farm consisting of two 2 MW Vestas V66 wind turbines. The site is located on the northeast coast of England, off the Northumberland shore. The turbines are located approximately 1 km from the shoreline. The mean water depth at the instrumented turbine varies between a lowest astronomical tide (LAT) level of 6 m and a mean high water springs (MHWS) level of 11 m; the average water depth is approximately 9 m. One of the two turbines (the southern turbine in Fig. 1) at Blyth was instrumented as part of a research project funded by the European Commission; it has a hub height of 62 m above the LAT level and a blade diameter of 66 m. The turbines are located on sharply sloping submerged rock, known as the "North Spit," in rock-socket type foundations.

Field measurements were collected for 16 months between October 2001 and January 2003, thus covering more than one full winter season. Measured data included wind speed and direction (using an anemometer placed on the turbine's nacelle), sea surface elevation (using a wave radar mounted on the turbine walkway), and bending moments at several vertical stations along the tower and the pile. One of these stations—the mudline bending moment—is our load variable of interest here. Additional details regarding the data and measurement system may be found in the report by Camp et al. [5].

The joint PDF of $\mathbf{X}$ (V and H_s here) needed for the statistical extrapolation is the same as was used by Agarwal and Manuel [4]; a Rayleigh distribution for V (truncated below cut-in and above cut-out wind speeds so as to focus only on the turbine's operating state) and a two-parameter Weibull distribution for H_s given V are assumed. Figure 2(*a*) shows that, at this site, V and H_s are correlated to varying degrees for winds from the sea and from the shore, and that wave heights associated with winds from the sea are generally higher. In addition, the wind rose in Fig. 2(*b*) shows the relative likelihood of winds from the sea versus winds from the shore and the distribution of available data according to wind direction for each wind regime. All of the information in Figs. 2(*a*) and 2(*b*) are employed in establishing $f_{\mathbf{X}}(\mathbf{x})$.

As part of the campaign data, time series for turbine loads in 10 min segments sampled at 40 Hz were recorded when a predetermined set of trigger conditions were met. The triggers for normal operating conditions were related to variations in the mean wind speed and direction, significant wave height, and tidal water level. Several other trigger conditions were defined in terms of the turbine state (operating, idling, startup, and shutdown), and extreme environmental events that included wind speeds above 25 m/s and significant wave heights above 4 m (Camp et al., [5]). In this study, we focus only on the data recorded during the normal operation of the turbine. In addition to the time-series data, minimum, maximum, mean, and standard deviation values for each channel were recorded as part of the statistics comprising the "summary" data sets (studied by Agarwal and Manuel [4]). The distribution of the usable data of the two types is summarized in

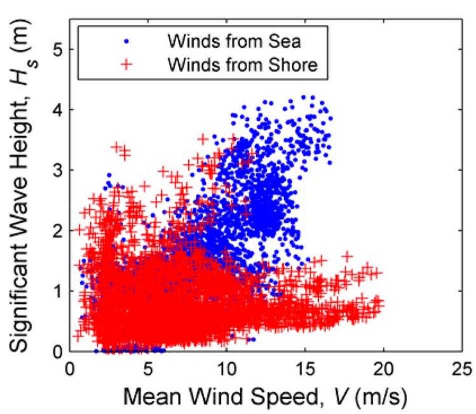

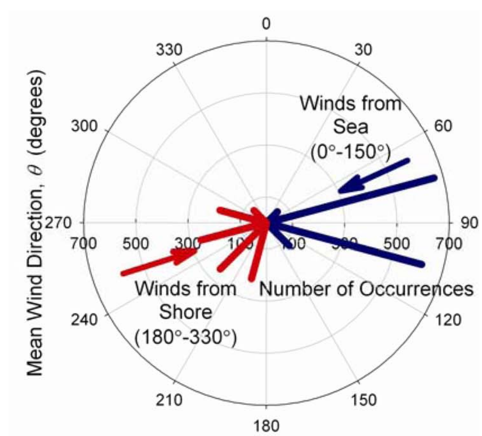

Fig. 2 (*a*) Scatter diagram showing mean wind speed versus significant wave heights; (*b*) wind rose

Table 1 Number of usable 10 min summary data sets and 10 min campaign data sets from the Blyth campaign

Data type	Winds from the sea	Winds from the shore	Winds from all directions
Summary	1398	903	2301
Campaign	646	368	1014

Table 1. Figure 3 shows the distribution of the available campaign data according to mean wind speed and significant wave height for winds from the sea and from the shore.

Representative Short-Term Response

We are interested in the response of the turbine while it is in an operating state as a function of wind speed and wave height both for winds from the sea and from the shore. Here, we select one time series each for the winds from the sea and from the shore, for which the largest mudline bending moment was recorded; these are referred to as ShoreV18H0N1 and SeaV12H3N41, respectively. The notation V*i*H*j*N*k* here refers to a time series from a bin bounded by mean wind speeds between i and $(i+2)$ m/s and significant wave heights between j and $(j+1)$ m; the notation N*k* represents the *k*th time series from this bin. The prefix "Shore" and "Sea" refer to winds from the shore and sea, respectively. Statistics for the wind, waves, and mudline bending moment for these two time series are summarized in Table 2 (one additional time series, referred to as ShoreV18H0N9, is also discussed in the table for comparison purposes).

Table 2 shows that the 10 min extreme mudline bending moments are 23.3 MN m and 19.4 MN m for the time series, ShoreV18H0N1 and SeaV12H3N41, respectively. The largest load during the campaign was recorded for winds from the shore. It is also found that turbine loads are primarily influenced by wind speed and only very slightly by wave height variation. It can also be seen from Table 2 that the mean wind speed recorded at the nacelle for time series, ShoreV18H0N1 and SeaV12H3N41, are 19.1 m/s and 13.2 m/s, respectively. Both these mean wind speeds are above the rated wind speed of 12 m/s for this turbine. More interesting is the difference in the standard deviations of the wind speed for these two time series. The turbulence standard deviation for the campaign ShoreV18H0N1 is more than twice the value observed for the campaign SeaV12H3N41. We point out here that wind speed measurements at the nacelle are likely affected by the turbine wake. Only the mean wind speed from the nacelle data was corrected for the free field mean wind speed (Camp et al. [5]); hence, the turbulence standard deviation at the nacelle may not give an accurate estimate of the turbulence character at hub height. Hence, we also compare turbulence standard deviations from another measurement of wind speed at a meteorological mast located on the shore (Fig. 1). These measurements were, however, at a height of 40 m, which is lower than the hub height of 62 m, and also this met. mast is about 1 km away from the turbine. Still, if either the nacelle or the met. mast data are considered, the turbulence standard deviation for data segments for winds from the shore is larger (by a factor of more than 2) than that for the data segment for winds from the sea. Since turbulence standard deviation (or equivalently, the turbulence intensity, which is the turbulence standard deviation divided by the mean wind speed) directly influences turbine loads, we might expect then that the largest loads will result during conditions associated with winds from the shore and will likely occur for higher wind speeds there.

Figure 4 shows time series and power spectral density (PSD) functions for the wind speed data (from both nacelle and met.

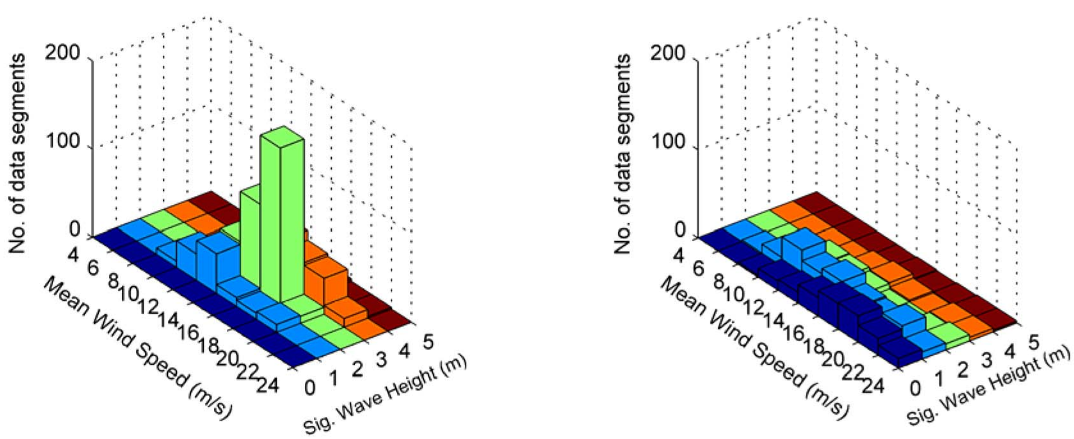

(a) (b)

Fig. 3 Distribution of usable campaign data sets by mean wind speed and significant wave height bins for (*a*) winds from the sea and (*b*) winds from the shore

Table 2 Statistics of the environment and load time series for the three selected campaigns shown in Fig. 4 (Note: SD: Standard deviation, H_s: Significant wave height)

	Wind speed (m/s)					Mudline bending moment	
	Nacelle		Met. Mast				
Selected time series	Mean	SD	Mean	SD	Sea surface elevation H_s (m)	Extreme (MN m)	Peak PSD ordinate ((MN m)^2/Hz)
ShoreV18H0N1	19.1	4.0	15.5	3.6	0.64	23.3	29.3
ShoreV18H0N9	18.6	2.4	13.9	2.2	0.64	14.9	4.2
SeaV12H3N41	13.2	1.8	12.7	1.7	3.47	19.4	1.0

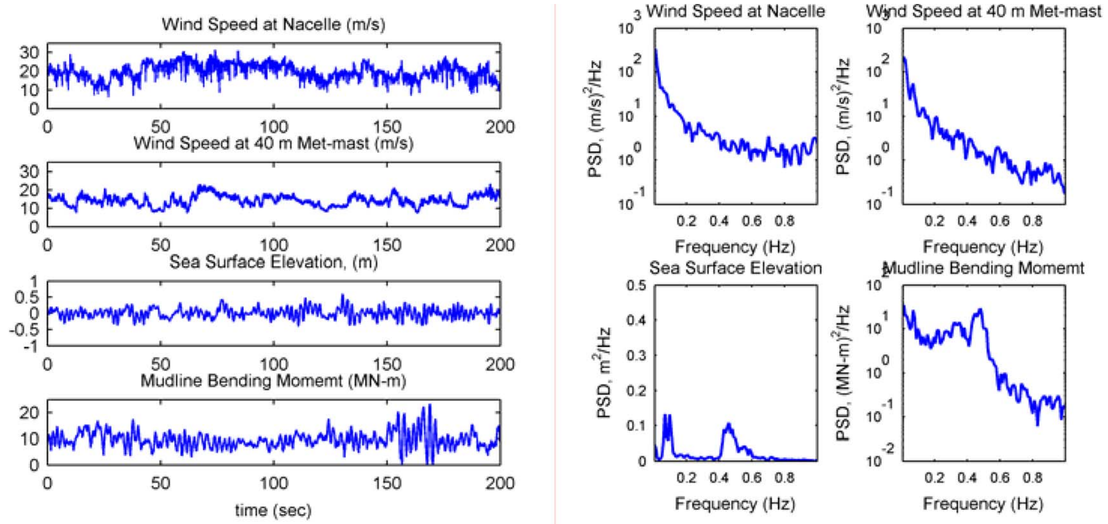

(a)

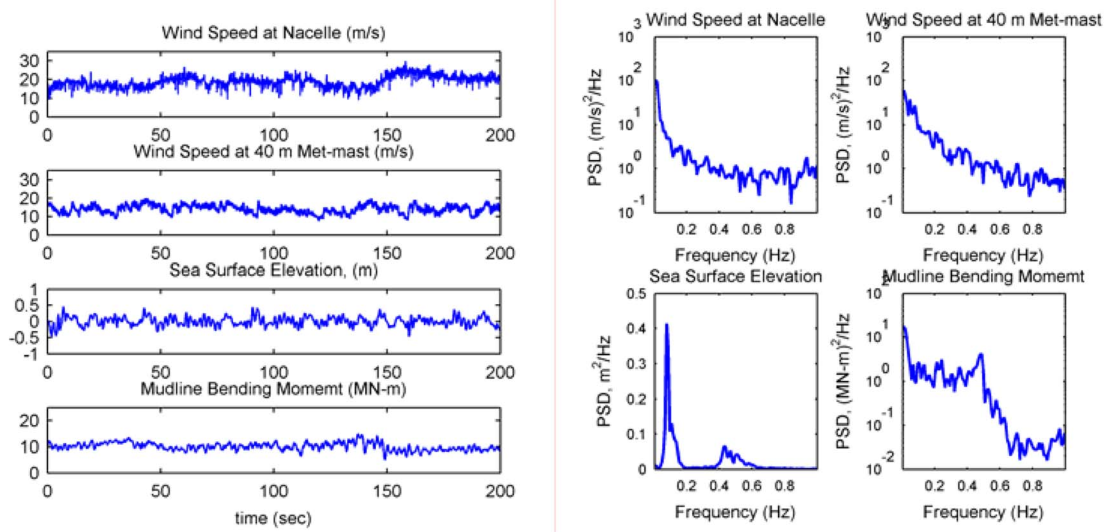

(b)

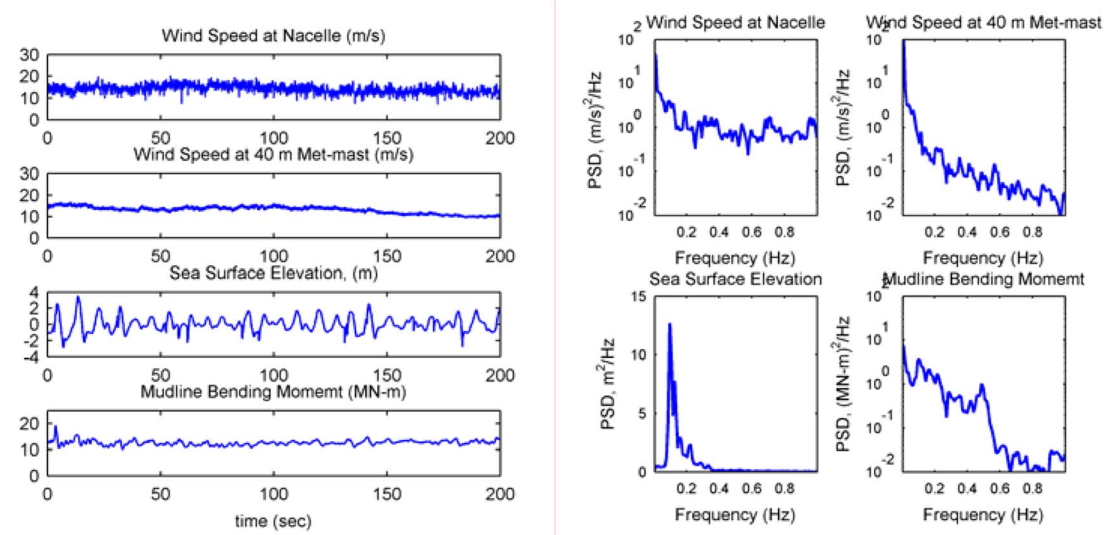

(c)

Fig. 4 Time series and power spectra of the wind speed at nacelle and met. mast, sea surface elevation, and mudline bending moment for the following 10 min time series: (*a*) ShoreV18H0N1, (*b*) ShoreV18H0N9, and (*c*) SeaV12H3N41. Only a 200 s portion is shown for each time series where the maximum load was recorded.

mast), the sea surface elevation, and the mudline bending moment for the three selected time series. For the time series, only a 200 s segment is shown where the largest load was recorded in each case. As expected, the nacelle turbulence time series and power spectra show more high-frequency content than is seen from the met. mast data; this is probably due to turbine wake effects. Comparing Figs. 4(*a*) and 4(*b*)—both for winds from the shore—it is seen that for these two time series with comparable mean wind speeds, turbine loads are higher when the turbulence intensity is higher (thus, ShoreV18H0N1 in Fig. 4(*a*) has higher loads than ShoreV18H0N9 in Fig. 4(*b*)). Both ShoreV18H0N1 and ShoreV18H0N9 have comparable significant wave heights and both also have comparable sea surface elevation PSD peaks at the tower natural frequency (approximately, 0.5 Hz); clearly, since ShoreV18H0N1 has the larger turbulence intensity, wind is the more important contributor to turbine loads than waves. Still, resonant vibrations of the tower are at least somewhat contributed to by waves and it is clear from studying Fig. 4(*a*), for example, that the largest loads in the mudline bending moment time series are recorded between 150 s and 200 s where the load process is oscillating at a frequency of around 0.5 Hz or a period of 2 s where waves provide some energy.

To summarize, for the two cases associated with winds from the shore, the ShoreV18H0N1 case where the turbulence standard deviation is 3.6 m/s (at the met. mast) compared to 2.2 m/s for the ShoreV18H0N9 case, experiences the larger load of 23.3 MN m compared to 14.9 MN m in the other case.

Figure 4(*c*) shows similar time series and PSD estimates for a data segment associated with winds from the sea, SeaV12H3N41, as were studied in Figs. 4(*a*) and 4(*b*) for the cases with winds from the shore. The largest recorded load for winds from the sea occurred for the selected data segment. As was discussed earlier, winds from the sea are less turbulent than winds from the shore; here, for example, turbulence standard deviations are only 1.7 m/s at the met. mast compared to the values of 3.6 m/s and 2.2 m/s, respectively, for the cases for winds from the shore, ShoreV18H0N1 and ShoreV18H0N9. As a result, despite the fact that the significant wave height for SeaV12H3N41 is considerably larger than for ShoreV18H0N1, the extreme turbine loads are smaller for this case (19.4 MN m) compared to 23.3 MN m for ShoreV18H0N1. Again, we reiterate that turbulence has primary influence on turbine loads and waves have only secondary influence.

While only three 10 minute time series were selected here to illustrate differences between winds from the sea and the shore and their influence on turbine loads, the conclusions reached from studying these, namely, that winds from the shore cause larger loads due to their higher turbulence intensities and that wind speed is more important than wave height, are supported when one studies other data segments in the campaign as well. Next, we derive turbine long-term loads based on short-term extreme load distributions based on POT analyses of all the available time series data.

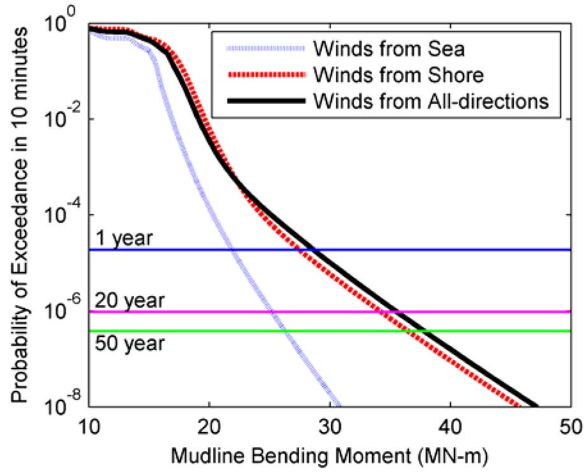

Fig. 5 Probability of load exceedance curves for winds from the sea, winds from the shore, and winds from all directions

Long-Term Turbine Loads

Based on Eq. (1), we now discuss derivation of long-term design loads based on first establishing short-term (conditional) load distributions of the load given V and H_s for all the wind-wave combinations associated with winds from the sea and from the shore. Using the extreme loads POT data, a three-parameter Weibull fit is applied for each V-H_s bin to yield the short-term distributions.

Figure 5 shows probability of load exceedance curves for winds from the sea, winds from the shore, and winds from all directions. It is clear that winds from the shore govern the long-term design loads for almost all return periods. Also, design loads based on winds from all directions are almost the same as those based on winds from the shore. This is because at longer return periods, the exceedance probability (of specified load levels) for winds from the shore is about two orders of magnitude higher than that for winds from the sea and, thus, the exceedance probability for winds from all directions, which represents the sum of these probabilities for winds from the sea and from the shore, is almost same as that for the winds from the shore alone.

The present study was based on the use of campaign data (i.e., time series data) to which the POT method was applied to yield short-term load distributions that were then used with Eq. (1) to yield the curves shown in Fig. 5. In an earlier study, Agarwal and Manuel [4] used summary data (only global maxima were considered) and similar curves were developed there. Table 3 shows a comparison of 1 and 20 year design loads from these two studies. The present study yields consistently smaller design load level. However, as is clear from the table, the 1 year loads from the present study, in all cases, were generally never more than 10% smaller and the 20 year loads never more than 15% smaller.

Table 3 Comparison of 1 and 20 year design loads (mudline bending moment in MN m) from this study and from Agarwal and Manuel [4]

	Winds from the sea		Winds from the shore		Winds from all directions	
Method	1 yr	20 yr	1 yr	20 yr	1 yr	20 yr
Present study (POT-based)	21.9	25.2	27.4	34.3	28.6	35.6
Agarwal and Manuel [4]	23.9	29.7	29.2	37.7	29.4	37.9

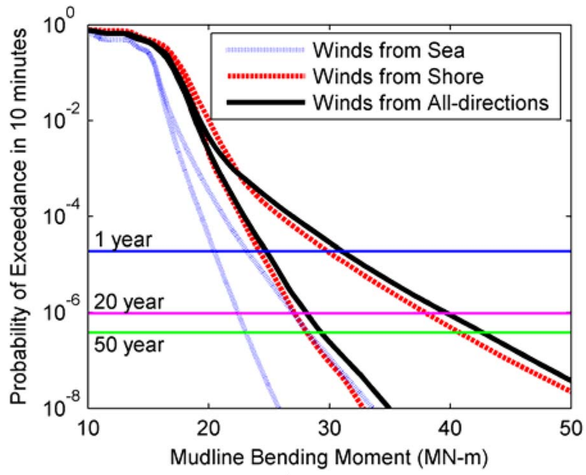

Fig. 6 90% confidence intervals on probability of load exceedance curves for winds from the sea, winds from the shore, and winds from all directions based on bootstrapping

Because the design loads derived as summarized in Fig. 5 and Table 3 are based on the use of limited data, there is uncertainty associated with their estimation. We employ nonparametric bootstrap techniques (Efron and Tibshirani [6]) that rely on randomly resampling with replacement the POT data and then estimating three-parameter Weibull parameters for the short-term load distributions in Eq. (1). Exceedance probability curves for each of the resamplings are then developed and can yield 5% and 95% levels of probability for a specified load level. These then represent 90% confidence intervals, as shown in Fig. 6. For instance, from Figs. 5 and 6, one can say that the 20-year mean design load is 35.6 MN m for winds from all directions but that there is a 90% chance that the 20 year design load may lie between roughly 29 MN m and 40 MN m. It is also noted that the confidence intervals for winds from the shore are larger than those for winds from the sea.

Conclusions

Our objective in this study was to derive long-term design loads for a 2 MW offshore wind turbine sited in 9 m of water at the Blyth site in the United Kingdom. Field data were available on wind speed, wave height, and mudline bending moment. Using time series data on the turbine load, the POT method was applied to develop load distributions given wind speed and wave height for winds from the shore and winds from the sea. Integration of these distributions along with the relative likelihood of different wind speed and wave height combinations allowed derivation of turbine long-term design loads.

The following represent some general conclusions based on the analyses conducted:

- Winds from the shore govern the design loads for the instrumented wind turbine at Blyth. A detailed analysis of available time series shows that winds from the shore result in larger loads, compared to winds from the sea, due to (1) the larger turbulence intensity associated with winds from the shore and (2) the relatively greater amounts of energy in the waves at the tower natural frequency (seen in a load time series studied that was associated with winds from the shore compared to one associated with winds from the sea).
- Design loads based on the POT method using the campaign data are reasonably close to those based on the global maxima method that were based on the use of summary data.
- Confidence intervals on turbine design loads, obtained using non-parametric bootstrap methods, are larger for winds from the shore.

Acknowledgment

The authors gratefully acknowledge the financial support provided by two grants from the National Science Foundation (CAREER Award No. CMS-0449128 and Award No. CMMI-0727989). They also thank Garrad Hassan and Partners for providing the data recorded at the Blyth site.

References

[1] IEC 61400-3, 2005, Wind Turbines—Part 3: Design Requirements for Offshore Wind Turbines, International Electrotechnical Commission, TC88 WG3 Committee Draft.

[2] Moriarty, P. J., Holley, W. E., and Butterfield, S. P., 2004, “Extrapolation of Extreme and Fatigue Loads using Probabilistic Methods,” National Renewable Energy Laboratory, NREL/TP-500–34421.

[3] Fitzwater, L. M., and Winterstein, S. R., 2001, “Predicting Design Wind Turbine Loads From Limited Data: Comparing Random Process and Random Peak Models,” *Proceedings of 2001 Wind Energy Symposium*, pp. 355–364.

[4] Agarwal, P., and Manuel, L. 2007, “On the Joint Wind-Wave Environment and Its Influence on Offshore Wind Turbine Loads,” *ASME Wind Energy Symposium*, Reno, NV.

[5] Camp, T. R., Morris, M. J., van Rooij, R., van der Tempel, J., Zaaijer, M., Henderson, A., Argyriadis, K., Schwartz, S., Just, H., Grainger, W., and Pearce, D., 2003, “Design Methods for Offshore Wind Turbines at Exposed Sites,” Final Report of the OWTES Project, Garrad Hassan and Partners Ltd., Bristol, UK.

[6] Efron, B., and Tibshirani, R. J., 1993, *An Introduction to the Bootstrap*, Chapman & Hall, New York.